THE JOURNAL OF PHYSICAL CHEMISTRY C

ARTICLE

pubs.acs.org/JPCC

Comparison of the Carbonyl and Nitrosyl Complexes Formed by Adsorption of CO and NO on Monolayers of Iron Phthalocyanine on Au(111)

Cristina Isvoranu,[†] Bin Wang,[‡] Evren Ataman,[†] Jan Knudsen,[†] Karina Schulte,[§] Jesper N. Andersen,[†] Marie-Laure Bocquet,[‡] and Joachim Schnadt*[,†]

[†]Division of Synchrotron Radiation Research, Department of Physics, Lund University, Box 118, 221 00 Lund, Sweden

[‡]Laboratoire de Chimie, Ecole Normale Supérieure de Lyon, 46, Allée d'Italie, 69364 Lyon Cedex 07, France

[§]MAX IV Laboratory, Lund University, Box 118, 221 00 Lund, Sweden

ABSTRACT: The interaction between monolayers of iron phthalocyanine on a Au(111) support and carbon monoxide and nitric oxide is studied by X-ray photoelectron spectroscopy and density functional theory calculations. We find several carbon monoxide and nitric oxide adsorbate species, and in particular species that bind to the iron ions of the phthalocyanine compound. The formation of phthalocyanine carbonyl and nitrosyl complexes leads to a redistribution of the electrons in the iron 3d levels resulting in a change of the spin state. Further, the adsorption results in an electronic decoupling of the iron phthalocyanine adsorbates from the substrate. The extent of the spin change and adsorbate−substrate decoupling depends on which ligand is used. The X-ray photoelectron spectroscopy results suggest that a covalent bond is formed between the NO and CO adsorbates and the FePc iron ion, and that the NO and CO valence states hybridize with metal ion d states. The density functional theory calculations show that CO adsorbs in a linear configuration, while NO adsorption assumes a tilted geometry.

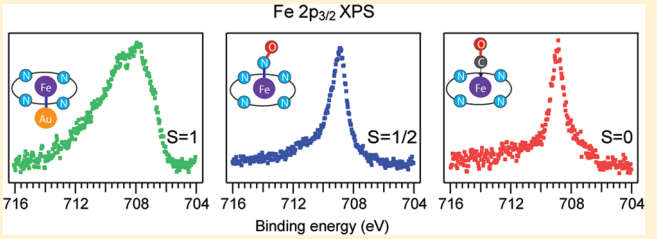

INTRODUCTION

Nitric oxide (•NO) and carbon monoxide (:CO) are diatomic molecules with unique and rich chemistry. They are both known to function as ligands in coordination complexes, some of which have extreme biological importance. Nitric oxide has one unpaired electron and is thus a highly reactive free radical species. It is a signaling molecule in many physiological processes in the human body (neurotransmitter, cytoprotective molecule, regulation of cardiovascular function),[1] actually being one of the smallest biologically active molecules. Some of the common reactions of NO involve heme-containing proteins; NO reacts with the metal center of the heme complex to form a nitrosyl complex. Carbon monoxide is a highly toxic gas, produced from the partial oxidation of hydrocarbons. Its acute toxicity stems from the fact that it binds irreversibly to the iron contained in the heme cofactor of the red blood cells,[2] with the consequence that the hemoglobin loses its oxygen carrying capacity. What makes CO chemistry unique is that even though the oxygen atom is the more electronegative species, it is the carbon atom that is the reactive part of the molecule and that binds to the metals when forming complexes.[3] The reason is to be sought in the complex distribution of the electrons forming the molecular orbitals, resulting in a localization of the highest occupied molecular orbital on the C atom.

Since NO and CO exert many of their effects by interacting with the metal center of the metalloprotein cofactor, it is important to develop a fundamental understanding of the metal−NO and metal−CO interactions. Of interest is also that the binding capacity of CO and NO to metal centers can be exploited for possible applications in gas sensing devices, catalysis, and, as suggested by the present results, molecular spintronics. With that in mind, we have chosen a model system with a structure that is similar to that of the biologically relevant porphyrin molecules, namely iron phthalocyanine (FePc), and studied the effects of adsorption of CO and NO on this system. The iron atom in the FePc molecules, the structure of which is shown in Figure 1, is in the Fe^{2+} oxidation state.

A number of theoretical (see, e.g., refs 4−10) and experimental (e.g., refs 11−18) papers have appeared in the literature, which deal with the issue of gas adsorption on phthalocyanines, porphyrins, and related molecules. Recently, particular interest has arisen in the influence of adsorption of small ligands on the spin state and magnetization of the macrocycle molecules.[19−24] Here we extend the scope of our previous work,[20−22] which is concerned with a comparison of the influence of adsorption of different ligands on the FePc spin state[20] and the detailed description of adsorption of ammonia and pyridine on a FePc monolayer,[21,22] and report on the atomic-scale details of adsorption

Received: May 12, 2011
Revised: October 9, 2011
Published: October 25, 2011

dx.doi.org/10.1021/jp204461k | J. Phys. Chem. C 2011, 115, 24718–24727

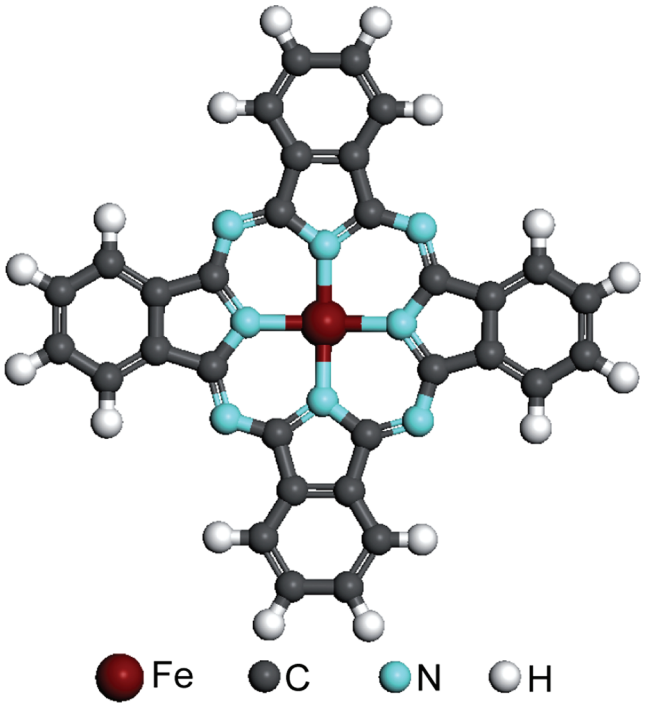

Figure 1. Molecular structure of iron phthalocyanine.

of CO and NO on monolayers of iron phthalocyanine on a Au(111) support. Using X-ray photoelectron spectroscopy (XPS) and density functional theory (DFT) we find that CO and NO bind axially to the iron ion of FePc. The metal−ligand bond results in the formation of carbonyl and nitrosyl complexes, with consequences for the spin state of the FePc and its coupling to the Au(111) substrate.

METHODS

The XPS experiments were carried out at the spectroscopy end station of beamline I311[25] of the Swedish national synchrotron radiation facility MAX-lab, Lund. The samples were prepared in the preparation chamber with a base pressure of 8×10^{-11} mbar, and the measurements were performed with a Scienta SES200 electron energy analyzer in the analysis chamber with a base pressure of 5×10^{-11} mbar. Monolayers of FePc were prepared by annealing at ∼380 °C multilayers of FePc obtained by vacuum sublimation (400 °C) of FePc onto a Au(111) substrate kept at room temperature. Prior to deposition, the FePc molecules (purchased from Sigma Aldrich, purity 90%) were degassed thoroughly for several days at ∼350 °C. The powder was further purified prior to evaporation by annealing it to 400 °C for approximately 3−4 h. The molecules were then deposited onto the crystal from a resistively heated tantalum pocket. Before that, the Au(111) single crystal had been cleaned by repeated cycles of sputtering and annealing. For sputtering 1 kV argon ions were used. Annealing was achieved by passing an electrical current through the tungsten wire holding the crystal until the temperature reached 500 °C. The sample was kept at this temperature for 10 min. The CO and NO adsorption experiments were carried out at a sample temperature of −253 °C. The gas doses ranged from 0.1 Langmuir (L) to 16 L (1 L = 10^{-6} Torr × s).

The C 1s, N 1s, O 1s, and Fe 2p photoemission spectra were recorded using photons with energies of 385, 525, 650, and 820 eV, respectively. During recording of the spectra the sample was continuously scanned in order to avoid beam damage. We used an overall instrumental resolution of 140 meV for the C 1s, 180 meV for the N 1s, 240 meV for the O 1s, and 280 meV for the Fe 2p XPS spectra. All spectra were calibrated with respect to the Fermi level of the sample. Polynomial-type backgrounds were subtracted from the Fe 2p, O 1s, and N 1s photoemission spectra. From the C 1s spectra, Shirley-type backgrounds were subtracted.

All DFT calculations were carried out with the VASP package[26] particularly adapted to simulate periodic interfaces. In the calculations we use the PBE-GGA[27] exchange-correction potential and the Ceperley-Alder version of the local density approximation (LDA).[28,29] The electron−core interactions were treated in the projector-augmented wave approximation.[30,31] We used a plane-wave cutoff energy of 400 eV and spin polarization. The Au substrate was modeled by an asymmetric slab with a four-layer (7 × 8) Au supercell. The FePc molecule was positioned above one side of the slab. In view of the large lateral dimensions of the periodic unit cell, the Brillouin zone was sampled with a single k-point at Γ-only. Both the molecule and the uppermost Au layer were free to relax until the self-consistent forces reached 20 meV/Å. The partial occupancies were treated with the method of Methfessel-Paxton[32] (0.2 eV smearing width). The Au bulk lattice constant was kept fixed at the calculated value of the uncovered metal, a = 4.17 Å with GGA or 4.06 Å with LDA. Both values are in good agreement with experimental results (a = 4.08 Å). The most stable configuration of FePc on Au(111) and the magnetic moments before and after gas adsorption were determined using both GGA and LDA functionals. Since the results from both functionals are very similar, the calculations shown in this paper refer to the PBE-GGA functional only (for more detailed discussion about all calculations performed, see ref 21).

RESULTS AND DISCUSSION

Fe 2p Photoemission and DFT Results. The Fe $2p_{3/2}$ photoelectron spectra shown in Figure 2 were obtained before and after dosing increasing amounts of carbon monoxide and nitric oxide on the Au(111)-supported FePc monolayers (for a characterization of the monolayer, see ref 21). The spectral changes are a result of bond formation between the FePc iron centers and CO and NO. In both cases, the changes are very similar: the lines become significantly narrower (cf. Table 1) and shift in binding energy. More quantitatively, the broad multiplet structure of the Fe $2p_{3/2}$ line of the pristine monolayer with a full width at half-maximum (fwhm) of 3.7 eV narrows to 1.1 eV (1.3 eV) after adsorbing an amount of CO (NO) corresponding to "iron saturation". Iron saturation is reached at a dose of 4 L, i.e., after this dose any increase in the amount of adsorbed gas does not lead to any further changes in the shape of the Fe $2p_{3/2}$ spectrum. At this dose, all FePc iron centers are bonded to ligand molecules, and there are no more iron binding sites available. As will be discussed later, the real saturation dose is actually somewhat lower than 4 L.

According to the literature, the type of bonds that CO and NO form with metals are very similar.[1,3] The molecular orbital structure of NO is similar to that of CO, but NO has an extra electron—the unpaired electron—in an antibonding π^* orbital.[33] The reactive atoms in CO and NO molecules are the C and N atoms, respectively. The metal−ligand bond is a special type of bond that can be described in terms of donation of electron density from the

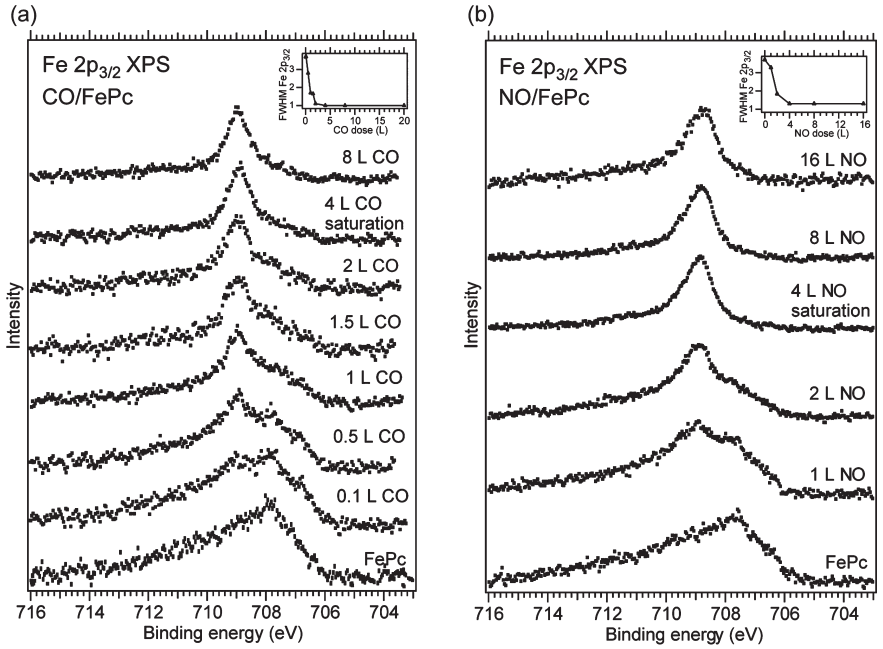

Figure 2. Fe $2p_{3/2}$ photoemission spectra before and after adsorbing increasing amounts of (a) CO and (b) NO on a monolayer of FePc on Au(111). The spectra are normalized with respect to the height of the most intense component. The spectra become narrower with increasing dose, up to the point where the signal reaches saturation, i.e., at 4 L dose. As described in the text, from the C 1s and N 1s spectra it can actually be inferred that the saturation coverage is reached at a dose between 2 and 4 L. The narrowing of the line is also accompanied by a shift toward higher binding energy. The inset in both spectra contains the evolution of the fwhm of the Fe $2p_{3/2}$ signal as a function of gas dose.

Table 1. Total fwhm of the Fe $2p_{3/2}$ Photoemission Line with Increasing the Amount of Adsorbed Gas[a]

CO adsorption		NO adsorption	
amount (L)	fwhm Fe $2p_{3/2}$ (eV)	amount (L)	fwhm Fe $2p_{3/2}$ (eV)
0.0	3.70	0.0	3.70
0.1	3.70	1.0	3.27
0.5	2.80	2.0	1.84
1.0	1.70	4.0	1.30
1.5	1.65	8.0	1.30
2.0	1.10	20.0	1.30
4.0	1.00		
8.0	1.00		
20.0	1.00		

[a] The uncertainty is ±50 meV.

CO and NO to the metal and back-donation from the metal d orbitals with appropriate symmetry and energy into antibonding ligand orbitals with π^* character.[34−36] The Fe−CO bond has coordinate character with both electrons involved in the direct CO−Fe donation originating from CO, while the Fe−NO bond is a conventional covalent-type interaction.[37]

The most drastic spectral change induced by the formation of the Fe−CO and Fe−NO bonds is the significant decrease in width of the Fe 2p line. It is well-known that the broad structure in the Fe 2p spectrum is caused by the open shell structure of the iron ion.[38−41] In previous studies[20−22] we have shown for a monolayer of FePc on Au(111) that the Fe 2p line receives additional broadening from the FePc−Au(111) interaction. In the following, we will argue that the decrease in the width of the Fe 2p line upon adsorption of the CO or NO ligand is a consequence of both a reduction of the valence spin and a weakening of the coupling between the FePc compound and the substrate.

Figure 3 shows the results of a least-squares fit of the Fe $2p_{3/2}$ photoemission spectrum of a clean FePc monolayer as well as that of the corresponding spectra at iron saturation after dosing CO and NO. The binding energies and fwhm's of the fitted peaks are provided in Table 2. The monolayer spectrum and the spectrum after CO adsorption were fitted by two main multiplet lines (P1 and P2) and a satellite[42,43] (P3) at ∼710−711 eV, while the spectrum after NO adsorption was fitted with one main line (P2) and the satellite only. The middle multiplet line of the monolayer (P2), in turn, was modeled by two peaks to account for the visible fine structure, while the low binding energy line (P1) and all the corresponding lines after CO and NO adsorption were modeled by one peak only since no detailed fine structure was visible. To a large extent, the width of the P1 and P2 lines (for the clean monolayer spectrum, the fwhm of the P2 line was obtained from considering a superposition of the two P2 peaks) is related to the splitting of the m_j components.[20,21,38−41] In line with previous work of ours,[20] we assign the low binding energy line (P1) of the FePc/Au(111) and CO/FePc/Au(111) samples to a component that results from charge transfer from the Au(111) substrate to the Fe atom in either the initial or final state. The reason for fitting the low-binding energy line in the monolayer spectrum with one peak only is justified by the fact that charge transfer from the substrate giving rise to this state is expected to lower the valence spin compared to the middle line and, consequently, the splitting between the m_j components. The low-binding energy line is very intense for the clean FePc monolayer as compared to its intensity for the CO sample and its complete disappearance after adsorption of NO. The reduced intensity of the P1 component upon gas adsorption indicates that

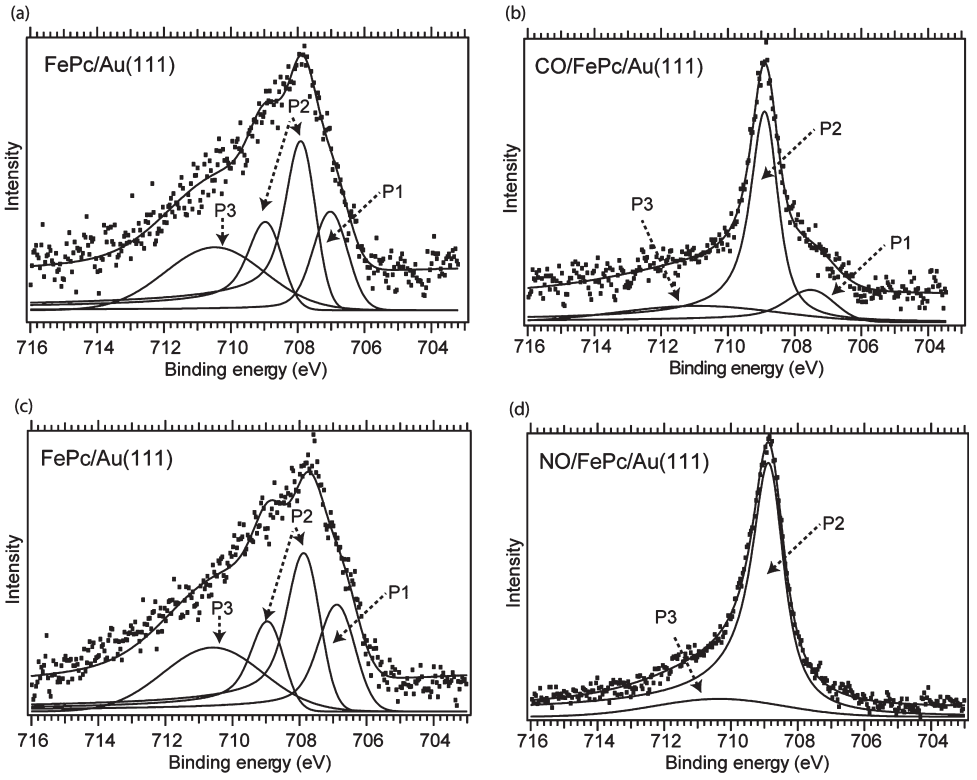

Figure 3. Fe $2p_{3/2}$ photoemission line (experimental data and fit) for (a,c) monolayer FePc/Au(111) (where panel a represents the monolayer onto which CO adsorption experiments were carried out and panel c is the monolayer onto which the NO adsorption experiments were carried out); (b) CO adsorption on monolayer FePc/Au(111) at saturation; (d) NO adsorption on monolayer FePc/Au(111) at saturation.

initially there is a strong coupling between the monolayer FePc adsorbates and the substrate, which is significantly reduced after CO adsorption and completely quenched after NO adsorption. The reason for the decoupling is found in the so-called *trans* effect,[44,45] in which two different ligands in trans position on a square planar or octahedral complex compete for the same (most likely d_{z^2}) orbital. This is especially relevant for the heme-like complexes, for which the proximity or absence of specific amino acid residues located near the heme molecule influences its ability to bind or release oxygen.

Now considering the middle component P2 at 708.19 eV for FePc/Au(111) (its binding energy was determined from a consideration of the superpositions of the of two peaks), 708.86 eV for CO/FePc/Au(111), and 708.81 for NO/FePc/Au(111), it is seen that its fwhm decreases from 2.02 eV for a clean FePc monolayer to 1.01 eV after CO and 1.25 eV after NO adsorption (cf. Table 2). Since, as outlined above, the fwhm is related to the Zeeman-like splitting of the m_j components in the field of the valence spin, we attribute the decrease in fwhm to a total valence spin quench after CO adsorption and a partial valence spin quench caused by NO adsorption. We have observed a similar effect for the adsorption of ammonia and pyridine on FePc.[21,22] The reduction in fwhm is accompanied by a shift of P2 to approximately +0.5 eV higher binding energy. Such a shift is not observed for adsorption of ammonia and pyridine.[21,22] It is a sign of the stronger interaction of CO and NO with the iron ion as compared to that of pyridine and ammonia. It has been shown experimentally that the interaction of CO with a metal surface leads to the formation of a covalent bond concomitant with a significant hybridization of the molecular valence states with parts of the metal d-band,[35] and the same effect is expected for the adsorption of CO (and NO) on metal ions.[46] Hence, the overall shift of 0.5 eV might be a combination of a chemical shift and a changed screening of the Fe 2p core hole.

The DFT results are in line with the conclusions drawn from the experiments, and, in particular, as discussed in detail below they confirm the conclusions regarding the change of valence spin of the FePc compound upon gas adsorption. The adsorbate-NO and CO geometries found in DFT are shown in Figure 4. They are based on FePc on Au(111) in a top-rotated configuration, which was found to be the most stable FePc configuration (for a more detailed discussion of the considered configurations of FePc see ref 21.). Clearly, a bond is formed between the iron center and the CO and NO ligands (Figure 4). The projected densities of states in Figure 5 furthermore support the idea of spin change after ligand adsorption.

Before going into the details related to the effects of adsorption of CO and NO, we would like to briefly discuss the system before gas adsorption. For FePc/Au(111), the interaction between the iron ion of FePc and the Au surface is covalent. The calculations show that the Au atom situated below the Fe is moved by ~0.4 Å from the Au surface toward the Fe iron and the Fe−Au distance is ~2.76 Å. While these absolute values may not be regarded as reliable, since dispersion interactions are not modeled by standard DFT code as used here, they nonetheless convey a qualitative impression of the effects of bond formation.

From the calculations we find significant changes in the electronic and geometric structure of FePc after adsorption of CO and NO on the iron ion (Figure 4). Bond formation between the Fe ion and CO and NO, respectively, takes place with the CO

(adsorption energy −1.40 eV/molecule) and NO (−1.83 eV/molecule) ligands in an axial position with respect to the FePc ring. The adsorption decouples the FePc molecules from the substrate, and the spin state of FePc is affected significantly by the new bonds. CO adsorbs in a linear geometry, while NO prefers a tilted geometry, in line with previous theoretical work.[1,6−9] The ligand-induced FePc-substrate decoupling is a consequence of the bonding between the ligands and the Fe ion, which induces a redistribution of the Fe 3d valence orbitals (Figure 5). We have observed the same kind of effect in studies concerned with the adsorption of ammonia and pyridine on FePc,[21,22] and it has also been observed in a study of adsorption of NO on a cobalt porphyrin compound.[47]

Table 2. Binding Energies and fwhm's for the Peak Components of the Fe $2p_{3/2}$ Photoemission Spectra of Monolayer FePc/Au(111), CO/FePc/Au(111), and NO/FePc/Au(111) at Saturation[a]

compound	peak	binding energy (eV)	fwhm (eV)
FePc/Au(111) monolayer for CO experiments	P1	706.99 ± 0.20	1.33 ± 0.20
	P2_1	707.81 ± 0.20	1.28 ± 0.20
	P2_2	708.84 ± 0.20	1.29 ± 0.20
	P2	708.19 ± 0.20	2.02 ± 0.20
	P3	710.48 ± 0.20	3.50 ± 0.20
FePc/Au(111) monolayer for NO experiments	P1	706.80 ± 0.20	1.34 ± 0.20
	P2_1	707.76 ± 0.20	1.24 ± 0.20
	P2_2	708.84 ± 0.20	1.26 ± 0.20
	P2	708.15 ± 0.20	2.08 ± 0.20
	P3	710.50 ± 0.20	3.50 ± 0.20
CO/FePc/Au(111)	P1	707.35 ± 0.05	1.84 ± 0.05
	P2	708.86 ± 0.05	1.01 ± 0.05
	P3	710.90 ± 0.05	5.67 ± 0.05
NO/FePc/Au(111)	P1	-	-
	P2	708.81 ± 0.05	1.25 ± 0.05
	P3	710.33 ± 0.05	4.53 ± 0.05

[a] For the middle monolayer line (P2), the parameters were obtained by considering the sum of the two peaks (labeled P2_1 and P2_2 in the table) used for fitting and determining the binding energy and fwhm of the resulting component.

The orbital redistribution also affects the iron spin state. The calculated magnetic moment for the FePc/Au(111) system is 2.36 μ_B with the GGA functional, which implies $S = 1$. This is consistent with previous theoretical and experimental results.[48−55] The calculated magnetic moment of FePc after adsorption of CO and NO is 0.09 μ_B and 0.84 μ_B, respectively. These theoretical results fully agree with our conclusions based on the experimental results of a complete spin quench upon CO and partial spin quench for NO adsorption. Both the spin quench and the decoupling of the FePc compound from the Au(111) substrate are reversible processes; the spin of the FePc molecule and the FePc−substrate bonding can be recovered by desorption of the ligands through warming of the sample.

Figure 5 shows the projected density of states (PDOS) on the iron *d* orbitals. The interaction of FePc with the Au(111) leads to a hybridization of the substrate states with the d_{z^2} orbital, which has the strongest *z*-direction component of all iron d-orbitals.

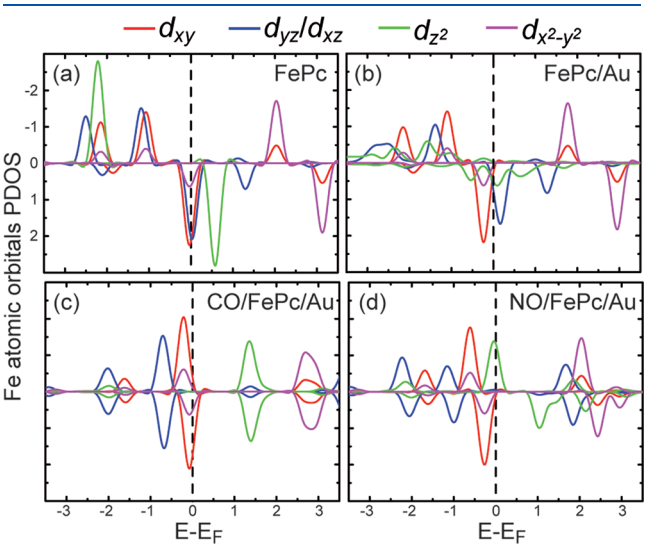

Figure 5. Projected density of states onto spin-up (positive) and spin-down (negative) states of (a,b) the d orbitals of the Fe atom in free and adsorbed FePc molecule, (c) the d orbitals of the Fe atom in adsorbed CO on FePc, and (d) the d orbitals of the Fe atom in adsorbed NO on FePc.

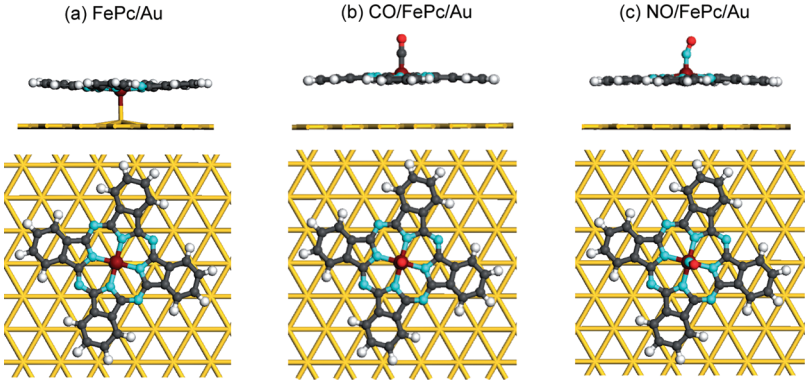

Figure 4. Optimized structures from DFT. (a) Top and side view of the most stable configuration of FePc on Au(111), the top-rotated configuration. (b,c) Top and side views of the system after adsorption of CO and NO, respectively. For the pristine FePc layer it is seen that a covalent bond is formed between the Fe ion of the FePc molecules and the Au(111) substrate. There is an upward motion of the Au atom beneath the iron atom of approximate 0.4 Å with respect to the average height of the Au(111) surface atoms. Upon adsorption of CO and NO the Au−Fe bond is released. Both CO and NO adsorb in axial position.

dx.doi.org/10.1021/jp204461k |*J. Phys. Chem. C* 2011, 115, 24718–24727

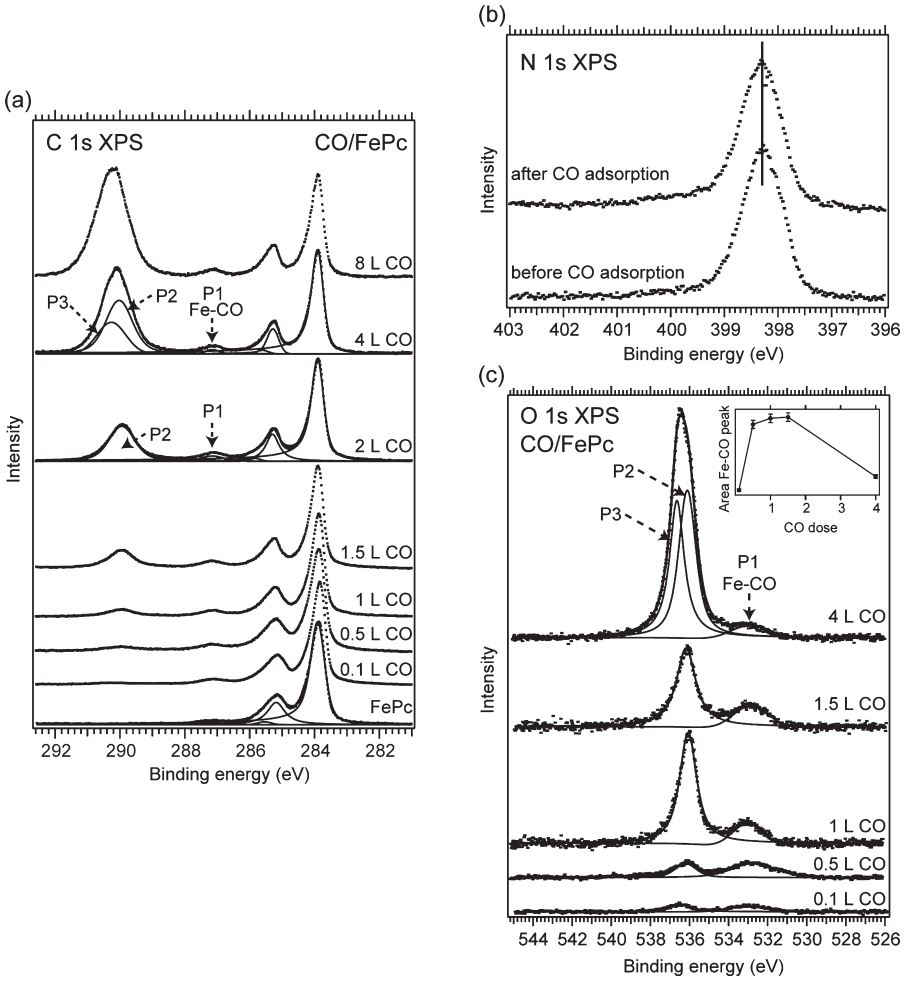

Figure 6. (a) C 1s photoemission lines before and after adsorption of increasing amounts of CO on the monolayer FePc/Au(111). The results of least-squares fitting performed is included for the spectra of the pristine FePc layer and after adsorption of 2 and 4 L. (b) N 1s photoemission spectra of the FePc monolayer before and after adsorption of CO. The N 1s core levels remain unchanged. (c) O 1s photoemission spectra (experimental data and fits). The inset shows how the area of the low-binding energy peak changes as a function of CO dose. The O 1s spectra show absolute intensity values; by contrast, the spectra in panels a and b are normalized with respect to the most intense peak.

The d_{yz} and d_{xz} orbitals are shifted in energy, while the $d_{x^2-y^2}$ and d_{xy} orbitals remain largely unchanged. The overall effect is a charge redistribution in the d orbitals, but the balance between spin-up and spin-down states is not changed significantly. In the presence of CO, the d_{z^2} states become narrower again as a consequence of the Fe−Au(111) decoupling. The other states are shifted, and as a consequence the relative populations of the spin-up and spin-down states are changed. In total, the spin on the iron ion is quenched, as seen from the symmetry between majority and minority spin states in Figure 5c. The d_{z^2} orbital is involved in this bond, as can be observed from the upward shift of the majority spin state at 1 eV above Fermi: the d_{z^2} becomes unoccupied. The NO bonding is quite different. Part of the d_{z^2} is found below the Fermi level, and the spin-up and spin-down components of the d_{z^2} orbital are not degenerate, and the antibonding part of the d_{z^2} orbital is broadened.

The different effect on the spin properties and on the adsorbate−substrate coupling caused by the binding of the CO and NO ligands to the iron shows an efficient way to tailor the electronic properties of the FePc compound on a Au(111) surface: the adsorbate−substrate coupling strength and the magnetic moment can be tuned differently by adsorption of different ligands on FePc.

N 1s, O 1s, and C 1s Photoemission. The C 1s, N 1s, and O 1s photoemission spectra before and after adsorption of increasing amounts of CO on the FePc/Au(111) sample are shown in Figure 6. The C 1s photoemission line of the FePc monolayer (Figure 6a, bottom spectrum) contains four peak components:[56−60] two main lines and two corresponding shakeup satellites, which are quite small and difficult to see in the figure. The main lines correspond to photoemission from the benzene carbon atoms (283.88 eV) and pyrrole carbon atoms, respectively (285.17 eV). The shake-ups are centered at 285.6 and 287.15 eV. CO adsorption results in a new peak at around 290 eV. At a CO dose of 4 L, two components can be assigned to this peak, P2 at 290.02 eV and P3 at 290.26 eV. P2 is assigned to first-layer CO molecules because it is also present at lower doses, while P3 first shows up at the dose of 4 L and is assigned to second-layer CO molecules. The peak at 287.15 eV (labeled P1), which coincides in position with the shakeup satellite of the pyrrole carbon atoms, becomes more intense after CO adsorption and develops in intensity up to the saturation point. Additional dosing does not

dx.doi.org/10.1021/jp204461k |J. Phys. Chem. C 2011, 115, 24718–24727

Table 3. Binding Energies (BE), fwhm's and Areas of the O 1s Photoemission Line Components (P1, P2 and P3) after Adsorbing Increasing Amounts of CO[a]

	P1			P2			P3		
dose	BE	area	fwhm	BE	area	fwhm	BE	area	fwhm
0.10	533.00	1.88	0.96	536.51	1.69	0.83			
0.50	532.73	5.67	1.16	536.2	2.91	0.71			
1.00	532.93	6.02	0.93	536.17	16.64	0.79			
1.50	533.05	6.09	0.95	536.08	20.18	0.68			
4.00	533.03	2.66	0.90	536.09	27.40	0.66	536.64	23.27	0.60

[a] The binding energy and fwhm uncertainty is ±50 meV. The dose is given in L; BE and FWHM are given in eV.

lead to any further increase in intensity. The observed intensity variation with dose implies that this peak contains a contribution from the CO molecules bound to iron (Fe−CO bonds). By subtracting the area of the monolayer pyrrole shakeup at 287.15 eV from the same peak corresponding to 4 L, we obtain the Fe−CO contribution to the peak. The area ratio between this contribution and the total area of the C 1s FePc peak is 1:32, which fits exactly to the stoichiometry of one CO molecule per FePc iron ion. The assignment is strengthened further by the fact that the position of the peak is in agreement with previously reported data on chemisorbed CO on metal surfaces.[61] With regard to the C 1s components related to the FePc compound, it is interesting to see that the pyrrole peak observed for the pristine FePc layer at 285.17 eV shifts to higher binding energy by 0.1 eV for the higher CO doses. A corresponding shift is observed neither for the benzene peak at 283.88 eV nor for the N 1s core level (Figure 6b). Still, this shift is small, and the interaction between the macrocycle part of the FePc molecule and CO is very weak.

Representative parameters from the least-squares fit of the O 1s data in Figure 6c are given in Table 3. Below a dose of 4 L CO, two peaks are found in the O 1s spectra: a low-binding energy peak at around 533 eV labeled P1 and a high-binding energy peak P2 at around 536.2 eV. As for the C 1s line, the formation of a second CO layer already at a dose of 4 L can be inferred from the occurrence of a high-binding energy component (P3) in the high-binding energy peak at 536.64 eV, which is attributed to molecules in the condensed CO multilayer. Consequently, P2 is assigned to CO molecules interacting with the FePc macrocycle, and the low-binding energy P1 peak is assigned to CO bonded to the FePc iron ions. The latter assignment is based on the development of the area of P1 (inset in Figure 6c), which increases strongly up to a dose of 1.5 L and then starts to be quenched at 4 L. The exact evolution of the area suggests that the multilayer starts to be formed at a dose somewhere between 1.5 and 4 L, which also implies that iron saturation is reached at the same dose. Finally, the possibility of CO molecules interacting with the Au(111) surface and contributing to P2 in both O 1s and C 1s spectra cannot be excluded.

Turning to the adsorption of NO on the FePc monolayer, Figure 7 shows the N 1s and O 1s photoemission spectra for different NO doses up to a dose, for which a multilayer of NO was formed. In Figure 7a also the N 1s spectrum for NO adsorption on the clean Au(111) surface is shown. Next to the low-binding energy N 1s peak at 398.2 eV related to the FePc compound, three peak features appear as a consequence of the NO adsorption. All these features are present from the lowest doses, and they are also present for multilayer NO. The N 1s spectrum of

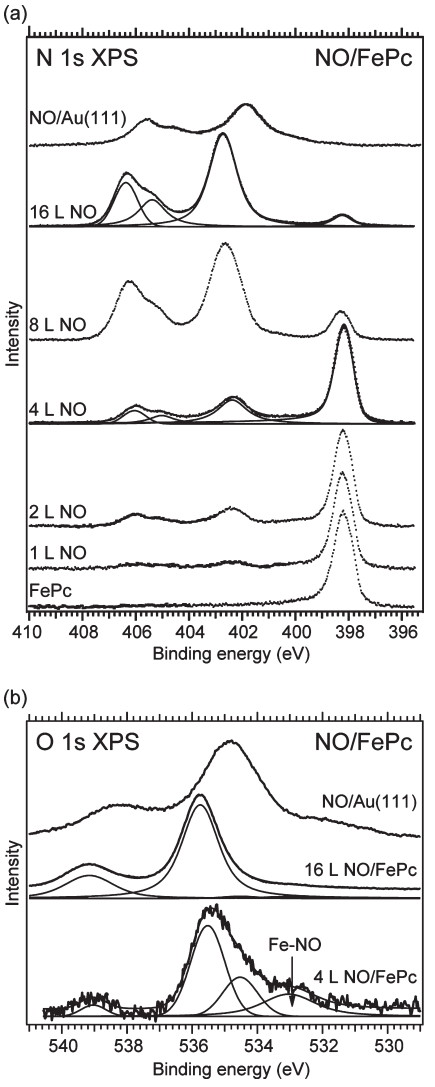

Figure 7. (a) N 1s photoemission spectra for increasing amounts of NO adsorbed on an FePc monolayer on Au(111). For 4 and 16 L the results of least-squares fitting are included. Each spectrum is normalized to the highest peak, except for the spectrum on bare Au(111), which was scaled so that its intensity is comparable to the spectrum on FePc at saturation. (b) O 1s photoemission signal: experimental data and results of the least-squares fits for the 4 and 16 L NO doses. The O 1s spectrum obtained after dosing NO on bare Au(111) is also shown.

NO on clean Au(111) shows the same peak features, but they are much broader and shifted by around 0.5 eV toward lower binding energy as compared to NO on FePc. The same finding applies to the O 1s spectrum for NO/Au(111) in Figure 7b. Least-square fits to the N 1s and O 1s spectra obtained after dosing 4 L NO (the dose at which the Fe 2p signal reaches saturation) and 16 L (corresponding to multilayer NO) are also shown in Figure 7. At 4 L dose, the NO N 1s peaks appear at 402.37, 405.02, and 406.04 eV. At 16 L, the N 1s signal of FePc is significantly attenuated, and the NO-related peaks are shifted by 0.35 eV to higher binding energy as compared to the 4 L dose. Since 16 L corresponds to a multilayer of NO, the higher binding energy is caused by a less efficient core-hole screening by the metallic substrate than in the case of thinner layers. At a dose of 4 L of NO, the O 1s peak at around 535.5 eV is significantly broader

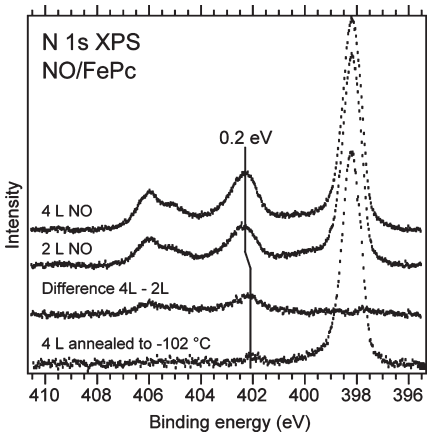

Figure 8. N 1s photoemission spectra for the doses of 4 and 2 L NO, difference of the 4 and 2 L spectra, and spectrum obtained after annealing the sample exposed to 4 L to −102 °C.

than at a dose of 16 L. More precisely, at 4 L dose the O 1s spectrum contains peaks at 533.03, 534.53, 535.52, and 539.03 eV. At 16 L dose, the intensity of the low-binding energy peaks at 533.03 and 534.53 eV is almost quenched, while the higher energy peaks at 535.52 and 539.03 eV are more intense and shifted by 0.23 and 0.13 eV to higher binding energies. The intensity quench of the two low-binding energy O 1s peaks at high NO doses indicates that the peaks are related to the Au(111)/FePc/NO interface. For adsorption of NO on a multilayer of FePc we also found the peak at the lowest binding energy[62] (in the multilayer case, it is situated at 533.16 eV), showing that this peak originates from the interaction between the Fe ions and NO. The peak at 534.53 eV, by contrast, was not observed for NO interacting with the FePc multilayer, and it is thus assigned to the direct NO/Au(111) interaction. Since the two highest-binding energy peaks are present both at low and high NO doses they are attributed to adsorption of NO on FePc on sites other than the iron, as well as to multilayer NO molecules.

The observation of multiple N 1s and O 1s peak features caused by NO adsorption is in agreement with literature data on porphyrins on a Ag(111) substrate,[63] but an exact assignment of the peaks has not been established so far. In principle, different peaks might be caused by different adsorption sites for NO,[64,65] different NO species adsorbed on the surface,[66−69] or differences in core−hole screening mechanisms,[70,71] as suggested by the literature data on NO adsorption on metals. On metal surfaces, NO is known to undergo either dissociative adsorption, combined molecular and dissociative adsorption, or molecular adsorption only.[65,72] On Au(111), NO is expected to undergo molecular adsorption.[72,73] Since the N 1s and O 1s spectral features for NO/FePc/Au(111) are very similar to what is seen for NO adsorption on bare Au(111), we conclude that the adsorption on FePc is molecular as well. This implies that different species such as NO monomers and $(NO)_2$ dimers might coexist. One very important aspect to be mentioned is that the peaks at higher binding energy in the O 1*s* spectra (535.52 and 539.03 eV) and the N 1s peaks at 402.37, 405.02, and 406.04 eV have very similar peak shapes and relative intensities as data previously reported in literature[70,71] and assigned to different screening mechanisms in the NO dimer. Also the binding energy shift between the O 1s peaks and between the N 1s peaks at 402.37 and 406.04 eV fits with those previous assignments. From the available data we are not able to provide an exact assignment of the NO-related N 1s and O 1s peaks, but a comparison of the spectral line shapes with the literature data suggests that the NO molecules primarily adsorb as dimers both on the clean Au(111) surface and in the FePc multilayer. In contrast, both the interaction of NO with the FePc iron ion (O 1s peak at 533.03 eV) and the direct interaction of NO with the Au(111) surface (O 1s peak at 534.53 eV) in the NO/FePc/Au(111) system are characterized by the monomer form. This is seen from the absence of the high binding energy peaks expected for dimer adsorption.[70] The binding of NO to the Au(111) as a monomer can be rationalized from the availability of limited space only in between the FePc molecules.

Finally, the N 1s peak related to the Fe−NO interaction is most likely hidden below the lowest binding energy NO peak. From the difference spectra shown in Figure 8, it can be seen that the difference between the N 1s spectra corresponding to doses of 4 and 2 L exhibits a low-binding energy feature at 402.2 eV. We assign this peak to the formation of Fe−NO bonds. To further support this assignment, in Figure 8 we also show the N 1s spectrum obtained after annealing the sample exposed to 4 L to −102 °C. A peak at the same position with that in the difference spectrum is obtained, showing once more that this low binding energy N 1s feature is very likely related to the strongest adsorption-induced interaction, which is expected to be the covalent Fe−NO bond. The other peaks are due to physisorbed NO in different forms. The question to be raised at this point is whether NO adsorption on the Fe takes place in monomer or dimer form. Since both the interaction between the NO molecules in the dimer and the Fe−NO bonds involve the unpaired electron on the NO molecule, it seems unlikely that adsorption in Fe would occur as dimer. DFT calculations show that the second NO molecule adsorption on the Fe would not lead to a stable configuration, so we conclude that the NO species binding to iron most likely are monomers.

CONCLUSIONS

The adsorption of CO and NO molecules on a monolayer of FePc supported by a Au(111) surface has been studied. The adsorption leads to a rehybridization of the Fe 3d states and the formation of carbonyl and nitrosyl complexes. In both cases the spin state of the iron ion is changed, and this change of spin state is accompanied by a decoupling of the FePc adsorbates from the substrate. The influence of the CO ligand is more drastic than that of NO: adsorption of CO completely quenches the spin. For NO adsorption, only a reduction of spin is observed, and this is related to the presence of the unpaired electron of the NO molecule. Instead NO has a more pronounced effect on the FePc/substrate coupling. In this case, the spectral signature of coupling between the FePc adsorbates and support observed in the Fe 2p spectra of FePc monolayers on Au(111) is completely lost. Apart from the NO and CO molecules interacting with the iron, there are several adsorption species present already from the lowest amounts of dosed gas. In the case of NO, it seems that a considerable part of the NO molecules adsorb in the $(NO)_2$ dimer form. The results, which are in line with previous studies, indicate that a precise tuning of the bond strength and spin state of the FePc molecules by ligand attachment is within reach and is strongly dependent on the chosen ligand.

ACKNOWLEDGMENT

The authors would like to thank the MAX-lab staff for technical support. We would also like to acknowledge funding

from the European Commission through the MONET Early Stage Researcher Training Network (Grant MEST-CT-2005-020908) and from Vetenskapsrådet (VR, Grant Nos. 2004-4404 and 2010-5080).

REFERENCES

(1) Ignarro, L. J. *Nitric Oxide—Biology and Pathology*; Academic Press: San Diego, 2000.
(2) Kotz, J. C.; Treichel, P. M.; Townsend, J. M. *Chemistry and Chemical Reactivity*; Thomson Brooks/Cole: Belmont, CA, 2009.
(3) Shriver, D. F.; Atkins, P. W.; Langford, C. H. *Inorganic Chemistry*, 2nd ed.; Oxford University Press: Oxford/Melbourne/Tokyo, 1994.
(4) Kurtikyan, T. S.; Mardyukov, A. N.; Goodwin, J. A. *Inorg. Chem.* **2003**, *42*, 8489–8493.
(5) Tran, N. L.; Kummel, A. C. *J. Chem. Phys.* **2007**, *127*, 214701.
(6) Radon, M.; Pierloot, K. *J. Phys. Chem. A* **2008**, *112*, 11824–11832.
(7) Ghosh, A.; Wondimagegn, T. *J. Am. Chem. Soc.* **2000**, *122*, 8101–8102.
(8) Ghosh, A. *Acc. Chem. Res.* **2005**, *38*, 943–954.
(9) Rovira, C.; Kunc, K.; Hutter, J.; Ballone, P.; Parrinello, M. *Int. J. Quantum Chem.* **1998**, *69*, 31–35.
(10) Bishop, S. R.; Tran, N. L.; Poon, G. C.; Kummel, A. C. *J. Chem. Phys.* **2007**, *127*, 214702.
(11) Dubey, M.; Bernasek, S. L.; Schwartz, J. *J. Am. Chem. Soc.* **2007**, *129*, 6980–6981.
(12) Praneeth, V. K. K.; Paulat, F.; Berto, T. C.; George, S. D.; Näther, C.; Sulok, C. D.; Lehnert, N. *J. Am. Chem. Soc.* **2008**, *130*, 15288–15303.
(13) Ma, X.; Chen, H.; Shi, M.; Wu, G.; Wang, M.; Huang, J. *Thin Solid Films* **2005**, *489*, 257–261.
(14) Newton, M. I.; Starke, T. K. H.; Willis, M. R.; McHale, G. *Sens. Actuators, B* **2000**, *67*, 307–311.
(15) Ho, K. C.; Tsou, Y. H. *Sens. Actuators, B* **2001**, *77*, 253–259.
(16) Basova, T. V.; Koltsov, E. K.; Igumenov, I. K. *Sens. Actuators, B* **2005**, *105*, 259–265.
(17) Palaniappan, A.; Moochhala, S.; Tay, F. E. H.; Su, X.; Phua, N. C. *Sens. Actuators, B* **2008**, *129*, 184–187.
(18) Maldonado, S.; García-Berríos, E.; Woodka, M. D.; Brunschwig, B. S.; Lewis, N. S. *Sens. Actuators, B* **2008**, *134*, 521–531.
(19) Stepanow, S.; Mugarza, A.; Ceballos, G.; Moras, P.; Cezar, J. C.; Carbone, C.; Gambardella, P. *Phys. Rev. B* **2010**, *82*, 014405.
(20) Isvoranu, C.; Wang, B.; Schulte, K.; Ataman, E.; Knudsen, J.; Andersen, J. N.; Bocquet, M.-L.; Schnadt, J. *J. Phys.: Condens. Matter* **2010**, *22*, 472002.
(21) Isvoranu, C.; Wang, B.; Ataman, E.; Schulte, K.; Knudsen, J.; Andersen, J. N.; Bocquet, M.-L.; Schnadt, J. *J. Chem. Phys.* **2011**, *134*, 114710.
(22) Isvoranu, C.; Wang, B.; Ataman, E.; Schulte, K.; Knudsen, J.; Andersen, J. N.; Bocquet, M.-L.; Schnadt, J. *J. Phys. Chem. C* **2011**, *115*, 20201–20208.
(23) Wäckerlin, C.; Chylarecka, D.; Kleibert, A.; Müller, K.; Iacovita, C.; Nolting, F.; Jung, T. A.; Ballav, N. *Nat. Commun.* **2010**, *1*, 1–7.
(24) Miguel, J.; Hermanns, C. F.; Bernien, M.; Kruger, A.; Kuch, W. *J. Phys. Chem. Lett.* **2011**, *2*, 1455–1459.
(25) Nyholm, R.; Andersen, J. N.; Johansson, U.; Jensen, B. N.; Lindau, I. *Nucl. Instrum. Methods Phys. Res. A* **2001**, *467−468*, 520–524.
(26) Kresse, G.; Furthmüller, J. *Phys. Rev. B* **1996**, *54*, 11169–11186.
(27) Perdew, J. P.; Burke, K.; Ernzerhof, M. *Phys. Rev. Lett.* **1996**, *77*, 3865–3688.
(28) Perdew, J. P.; Zunger, A. *Phys. Rev. B* **1981**, *23*, 5048–5079.
(29) Ceperley, D. M.; Alder, B. J. *Phys. Rev. Lett.* **1980**, *45*, 566–569.
(30) Blöchl, P. E. *Phys. Rev. B* **1994**, *50*, 17953–17979.
(31) Kresse, G.; Joubert, D. *Phys. Rev. B* **1999**, *59*, 1758–1775.
(32) Methfessel, M.; Paxton, A. T. *Phys. Rev. B* **1989**, *40*, 3616–3621.
(33) Shustorovich, E. M. *Zh. Strukt. Khim.* **1962**, *3*, 103–105.
(34) Blyholder, G. *J. Phys. Chem.* **1964**, *68*, 2772–2777.
(35) Nilsson, A.; Pettersson, L. G. M. *Surf. Sci. Rep.* **2004**, *55*, 49–167.
(36) Bennich, P.; Wiell, T.; Karis, O.; Weinelt, M.; Wassdahl, N.; Nilsson, A.; Nyberg, M.; Pettersson, L. G. M.; Stöhr, J.; Samant, M. *Phys. Rev. B* **1998**, *57*, 9274–9284.
(37) Albert, M. R.; Yates, J. T. *The Surface Scientist's Guide to Organometallic Chemistry*; American Chemical Society: Washington, DC, 1987.
(38) Weissenrieder, J.; Göthelid, M.; Månsson, M.; Schenck, von H.; Tjernberg, O.; Karlsson, U. O. *Surf. Sci.* **2003**, *527*, 163–172.
(39) Sirotti, F.; Santis, M. D.; Rossi, G. *Phys. Rev. B* **1993**, *48*, 8299–8306.
(40) Sirotti, F.; Rossi, G. *Phys. Rev. B* **1994**, *49*, 15682–15687.
(41) Fadley, C. S.; Shirley, D. A. *Phys. Rev. A* **1970**, *2*, 1109–1120.
(42) Bethke, C.; Kisker, E.; Weber, N. B.; Hillebrecht, F. U. *Phys. Rev. B* **2005**, *71*, 024413.
(43) Rossi, G.; Panacione, G.; Sirotti, F.; Lizzit, S.; Baraldi, A; Paolucci, G. *Phys. Rev. B* **1997**, *55*, 11488–11495.
(44) Hartley, F. R. *Chem. Soc. Rev.* **1973**, *2*, 163–179.
(45) Hieringer, W.; Flechtner, K.; Kretschmann, A.; Seufert, K.; Auwärter, W.; Barth, J. V.; Görling, A.; Steinrück, H. P.; Gottfried, J. M. *J. Am. Chem. Soc.* **2011**, *133*, 6206–6222.
(46) Nyberg, M.; Föhlisch, A.; Triguero, L.; Bassan, A.; Nilsson, A.; Petterson, L. G. M. *J. Mol. Struct.: THEOCHEM* **2006**, *762*, 123–132.
(47) Flechtner, K.; Kretschmann, A.; Steinrück, H. P.; Gottfried, J. M. *J. Am. Chem. Soc.* **2007**, *129*, 12110–12111.
(48) Hu, Z.; Li, B.; Zhao, A.; Yang, J.; Hou, J. G. *J. Phys. Chem. C* **2008**, *112*, 13650–13655.
(49) Gao, L.; Ji, W.; Hu, Y. B.; Cheng, Z. H.; Deng, Z. T.; Liu, Q.; Jiang, N.; Lin, X.; Guo, W.; Du, S. X.; Hofer, W. A.; Xie, X. C.; Gao., H.-J. *Phys. Rev. Lett.* **2007**, *99*, 106402.
(50) Bialek, B.; Kim, I. G.; Lee, J. I. *Surf. Sci.* **2003**, *526*, 367–374.
(51) Dale, B. W.; Williams, R. J. P.; Johnson, C. E.; Thorp, T. L. *J. Chem. Phys.* **1968**, *49*, 3441–3444.
(52) Barraclough, C. G.; Martin, R. L.; Mitra, S.; Sherwood, R. C. *J. Chem. Phys.* **1970**, *53*, 1643–1648.
(53) Reynolds, P. A.; Figgis, B. N. *Inorg. Chem.* **1991**, *30*, 2294–2300.
(54) Evangelisti, M.; Bartolomé, J.; de Jongh, L. J.; Filoti, G. *Phys. Rev. B* **2002**, *66*, 144410.
(55) Kuzmin, M. D.; Hayn, R.; Oison, V. *Phys. Rev. B* **2009**, *79*, 024413.
(56) Papageorgiou, N.; Salomon, E.; Angot, T.; Layet, J.-M.; Giovanelli, L.; Lay, G. L. *Prog. Surf. Sci.* **2004**, *77*, 139–170.
(57) Åhlund, J.; Nilson, K.; Schiessling, J.; Kjeldgaard, L.; Berner, S.; Mårtensson, N.; Puglia, C.; Brena, B.; Nyberg, M.; Luo, Y. *J. Chem. Phys.* **2006**, *125*, 034709.
(58) Peisert, H.; Knupfer, M.; Fink, J. *Surf. Sci.* **2002**, *515*, 491–498.
(59) Zhang, L.; Peisert, H.; Biswas, I.; Knupfer, M.; Batchelor, D.; Chassé, T. *Surf. Sci.* **2005**, *596*, 98–107.
(60) Isvoranu, C.; Åhlund, J.; Wang, B.; Ataman, E.; Mårtensson, N.; Puglia, C.; Andersen, J. N.; Bocquet, M. L.; Schnadt, J. *J. Chem. Phys.* **2009**, *131*, 214709.
(61) Sandell, A.; Bennich, P.; Nilsson, A.; Bernnäs, B.; Björneholm, O.; Mårtensson, N. *Surf. Sci.* **1994**, *310*, 16–26.
(62) Isvoranu, C.; Ataman, E.; Knudsen, J.; Schulte, K.; Wang, B.; Bocquet, M. L.; Andersen, J. N.; Schnadt, J. not published.
(63) Buchner, F.; Seufert, K.; Auwärter, W.; Helm, D.; Barth, J. V.; Flechtner, K.; Gottfried, J. M.; Steinrück, H.-P; Marbach, H. *ACS Nano* **2009**, *3*, 1789–1794.
(64) Zhu, Z. F.; Kinne, M.; Fuhrmann, T.; Denecke, R.; Steinrück, H.-P. *Surf. Sci.* **2003**, *529*, 384–396.
(65) Bertolo, M.; Jacobi, K. *Surf. Sci.* **1990**, *226*, 207–220.
(66) Pashutski, A.; Folman, M. *Surf. Sci.* **1989**, *216*, 395–408.
(67) Behm, R. J.; Brundle, C. R. *J. Vac. Sci. Technol. A* **1984**, *2*, 1040–1041.
(68) Brown, W. A.; Gardner, P.; King, D. A. *J. Phys. Chem.* **1995**, *99*, 7065–7074.
(69) Yoshinobu, J.; Kawi, M. *Chem. Lett.* **1995**, *24*, 605–606.
(70) Tonner, B. P.; Kao, C. M.; Plummer, E. W.; Caves, T. C.; Messmer, R. P.; Salaneck, W. R. *Phys. Rev. Lett.* **1983**, *51*, 1378–1381.

(71) Nelin, C. J.; Bagus, P. S.; Behm, J.; Brundle, C. R. *Chem. Phys. Lett.* **1984**, *105*, 58–63.
(72) Brown, W. A.; King, D. A. *J. Phys. Chem. B* **2000**, *104*, 2578–2595.
(73) McClure, S. M.; Kim, T. S.; Stiehl, J. D.; Tanaka, P. L.; Mullins, C. B. *J. Phys. Chem. B* **2004**, *108*, 17952–17958.